LRP 625/98 December 1998

APPLICATIONS OF THE CAVITY RING-DOWN TECHNIQUE TO A LARGE AREA RF-PLASMA REACTOR

F. Grangeon, C. Monard, J.-L. Dorier,
A.A. Howling, Ch. Hollenstein, D. Romanini,
N. Sadeghi

submitted for publication to
Plasma Sources Science & Technology

Applications of the cavity ring-down technique to a large area rf-plasma reactor

F. Grangeon[a)], C. Monard[a)], J.-L. Dorier[a)], A.A. Howling[a)], Ch. Hollenstein[a)], D. Romanini[b)], N. Sadeghi[b)]

a) Ecole Polytechnique Fédérale de Lausanne – Centre de Recherches en Physique des Plasmas, 1015 Lausanne, Switzerland

b) Laboratoire de Spectrométrie Physique (UMR 5588), Université Joseph Fourier de Grenoble, B.P. 87, 38402 Saint-Martin-d'Hères Cedex, France

Abstract.

The cavity ring-down technique is applied to an industrial-scale radio-frequency plasma reactor for the measurement of the density and spatial profile of negative ions in pure oxygen and hydrogen rf plasmas, and for the detection of nanometric particles in argon-silane plasmas. The real-time observation of powder formation is demonstrated to be feasible by the cavity ring-down technique. An observed plasma-induced spurious drift of the ring-down time is also studied and related to water desorption from the reactor walls and electrodes which is re-adsorbed on the mirror surfaces.

1. Introduction

The understanding of phenomena occurring in industrial rf plasmas is of great interest for the improvement of these processes and the resulting materials. Generally, the characterization of reactive plasmas requires non-intrusive techniques. In this way, optical diagnostics, and especially laser diagnostics, are powerful techniques. A few years ago, the Cavity Ring-Down technique was presented by O'Keefe and Deacon [1]. This diagnostic is based on the observation of the intensity decay of a laser light pulse trapped in a cavity formed by two high-reflectivity mirrors. One of the main advantages of this technique is its high sensitivity due to the multipass optical path; very low extinction coefficients (10^{-8}-10^{-5} cm^{-1}) can be measured, and therefore allowing detection of species at trace concentration [2].

The Cavity Ring-Down (CRD) technique has been used for the spectroscopy of species seeded in supersonic jets [3], for the investigation of reaction kinetics [4], for the detection of transient species in flames, reactors and discharges [5-7]. The observation of absorption lines of molecules such as CN, C_2H_2 and SiH_2 in gases and plasmas was also performed [8-10]. Until now, this technique has been applied only to laboratory plasma reactors. It seems that the CRD diagnostic could be employed for the characterization of plasmas in industrial-like conditions. Due to its high sensitivity, the CRD technique could be employed to determine additional characteristics such as negative ion density by photodetachment [11] or trapped nano-particles in rf plasmas by light absorption [10].

This paper investigates the feasibility of using the cavity ring down technique in an industrial plasma reactor. We will show here the determination of the negative ion density in pure oxygen and hydrogen plasmas, and the observation of nano-particles trapped in silane plasmas. We will also discuss results concerning an observed long-term plasma-induced drift of the ring down decay time.

2. Experimental set-up

The experimental set-up is shown in figure 1. The rf plasma box reactor is a Balzers Kai1 [12] which is formed by two rectangular electrodes (47 x 67 cm), with a gap of 24 mm, inside a vacuum chamber evacuated to a pressure about 1.10^{-6} Torr by a turbo-pump, and by a root pump during the process. The reactor pressure was controlled by a butterfly valve from 0.075 to 0.4 Torr. Fluxes of different gases (Ar, O_2, H_2, SiH_4, SF_6) are controlled by mass flowmeters. The excitation frequency is 13.56 MHz, and the power dissipated in the plasma can be up to 120 W for the experiments reported here.

The ring down cavity consists of two high reflectivity dielectric mirrors (> 99.99% in the 510 – 620 nm range, 1m radius of curvature, 7.75 mm diameter) in vacuum. In order to avoid instabilities of the confocal arrangement, the distance between the mirrors is 120 cm of which the plasma width occupies about 39% of the path length. A pulsed dye laser (Lambda Physik Scanmate 2EC filled with Rhodamine 6G, tuned at 566 nm, operated at 10 Hz, 4 ns pulse duration, about 1 mJ/pulse) is introduced into the back face of the entrance mirror. About 10^{-4} of the incident energy is therefore coupled by the entrance mirror into the cavity. The cavity diameter (i.e. the probe beam waist) is defined by the laser beam diameter and is about 3 mm. The mirror angle can be fine-tuned under vacuum by adjusting screws. The vertical position of the mirrors can be set by means of sliding vacuum-seal micrometer scale, allowing to make vertical density profiles between the electrodes. The output signal is measured behind the exit mirror by a Philips XP2020Q photomultiplier, acquired by a digital oscilloscope (Lecroy 9450), averaged over 200 shots, and analyzed by a Labview program on an Apple G3 computer. The real time measurements are performed by analysing the evolution of the ring down decay time with time. In this case, the signal is continuously averaged over 15 shots.

The output intensity I decays exponentially. The Labview program performs a non-linear Levenberg-Marquardt fit ($I=I_0\exp(-\tau/\tau_0)+I_{offset}$) to determine the exponential decay time τ (usually about 20 μs which

corresponds to 4000 passes). The presence of absorbing species in the cavity causes a decrease in the decay time. First, the decay time of the cavity without plasma, τ_0, is determined. After that, the decay time τ, in various plasma conditions, is measured. The extinction coefficient of the plasma at the laser wavelength is:

$$\alpha_{ext} = 1/c.(1/\tau - 1/\tau_0).L/d$$

where c is the speed of light, L is the cavity length and d is the length occupied by the plasma. If the cross-section σ of a process (photodetachment, excitation, or absorption by micro-particles) is known, the number density of the species can be determined:

$$N = \alpha_{ext}/\sigma$$

provided that the mechanism of absorption can be positively identified by supplementary information such as spectral scanning or, as shown here, by vertical profile measurements.

In practice, the ring-down time was observed to drift over several hours. The cause is due to degassing of the reactor walls as explained in section 3-(c). Reducing this drift is thus of great importance in order to perform reproducible measurements.

3. Results

a) Photodetachment in pure O_2 and H_2 plasmas

A discharge in oxygen causes a perfectly reproducible decrease in the decay time. This occurs abruptly on plasma ignition and recovers on plasma extinction. This decrease is a function of the plasma power, but is independent of the laser wavelength in the dye range (spectral range 555 – 585 nm). This effect was already observed in He-Ne laser multipass experiments in H_2 plasmas [11], and attributed to photodetachment of negative ions, leading to a measurable extinction coefficient. It is important to note that the attachment energy for O^- is about 1.463 eV and about 0.44 eV

for O_2^- molecules, and is thus lower than the photon energy at 566nm (2.15 eV) [13]. As a consequence, a single-photon photodetachment process on negative ions is then possible. Ionisation and dissociation processes on neutral species or positive ions are not possible since their energy thresholds are greater than the photon energy (dissociation energy: 5.12 eV for O_2 molecules, ionisation energy: 12.14 eV for O_2 molecules, 13.61 eV for O atoms) [13]. Photodetachment of negative ions is thus the most probable absorption process within this spectral range.

A vertical profile of the extinction was obtained by changing the position of the cavity between the electrodes. Figure 2 shows the variation of α_{ext} with the distance to the rf electrode, for different plasma powers. The profile exhibits a typical bell-shaped distribution for negative ions in rf plasmas with a maximum in the center of the plasma and a negligible density at the sheaths. This kind of distribution has already been observed [13, 14] and shows unambiguously that the observed extinction is due to photodetachment of negative ions.

It is known that the negative ions in pure O_2 rf discharges are mostly O^- ions (about 90%) [15, 16]. Since the photodetachment cross-section of O^- ions is about $6.3.10^{-18}$ cm^2 at the laser wavelength [17], it is possible to determine the negative ion density. The measured density mid-way between the electrodes (12 mm) is about 10^{10}-10^{11} cm^{-3} and is shown as a function of the input plasma power for different pressures in figure 3. The density increases quasi-linearly with the input power, but decreases when the pressure increases. The gas flow rate had no observable influence on the negative ion density. These trends are in good agreement with experimental and numerical results dealing with negative ion in oxygen rf discharges [18, 19].

These experimental results were compared with numerical calculations from the Kinema SIGLO-RF software [20]. Figure 4 presents the comparison of a calculated profile with experimental results, at the same rf voltage amplitude of 430 V, corresponding to a measured rf power of about 120 W, at a pressure of 0.1 Torr. We have observed a good qualitative and quantitative agreement between experiments and calculations. This confirms that the

observed decrease of the ring-down time is due to photodetachment on negative ions

Figure 5 shows the dependence of the density of negative ions on the plasma power, for different pressure conditions, in pure hydrogen plasmas. The anion present in H_2 rf plasmas is the H^- ion [13]. In the case of H atoms, the electron affinity is about 0.754 eV [13], and photodetachment is possible. Since the photodetachment cross-section is known to be $3.4.10^{-17}$ cm^2 at the laser wavelength [21], the negative ion density has been estimated to be about 10^9-10^{10} cm^{-3} in our plasma conditions. As in oxygen plasmas, the density increases when the power is increased or when the pressure is decreased.

Ring-down measurements were also made in pure SF_6 plasmas. Calculations with the SIGLO-RF software allowed us to estimate the negative ion density to be about 10^{10} cm^{-3}. Despite this, the SF_6 plasma has shown no observable absorption at the laser wavelength range. In SF_6 plasmas, SF_6^- ions are unstable and the electron affinity can be as high as 3.45 eV for F^- ions [13]. Only ions with electron affinity less than the photon energy (2.15 eV) can be detached by a single photon process at 566 nm. These ions present probably a low density in our plasma conditions (< few 10^9 cm^{-3}). As a consequence, no photodetachment is visible in SF_6 plasmas at the laser wavelength.

A photodetachment experiment can be perturbed by negative ion depletion, when most of the negative ions are photodetached [22]. In these experiments, we have assumed up until now that the depletion of negative ions is a negligible effect. This is confirmed by the following simple model: for our cavity (3 mm diameter), the residence time of an oxygen atom is about 5 μs and is equivalent to 1250 passes of the laser beam. This means that a negative ion is present 5 μs in the cavity and is replaced by a new ion after this time. During this time, the laser beam crosses about 6.10^4 cm in the plasma (1250 passes x 47 cm length). Considering an absorption coefficient about 10^{-7} cm^{-1}, this means that about 6.10^{-3} of photons present in the ring-

down cavity are lost by one-photon photodetachment process on negative ions. Considering a reflection coefficient of the entrance mirror larger than 99.99%, the energy of the laser beam coupled inside the cavity is less than 10^{-7} J. Therefore, the photon number trapped in the cavity is less than 5.10^{11}. As a consequence, during the residence time of the ions, about 3.10^{9} ions are photodetached. The number of ions present in the cavity is about 3.10^{10} (volume of plasma in the cavity x ion density). This means that less than 10% of the negative ions are detached during the residence time of ions. This is an upper limit since here we have neglected cavity losses and re-creation of negative ions by attachment during this time. A more complete model has been developed [23] and is in good agreement with this estimation.

The preceding results show the validity of the cavity ring-down technique for the measurement of negative ion density by a photodetachment process for rf discharges in electronegative gases. The principal advantages of the CRD technique are that it is a highly sensitive and non-intrusive diagnostic.

b) Powder detection in silane plasmas

One of the main topics in the study of deposition plasmas is the characterisation of nanometer-size particles created and trapped in the plasma [24]. Clusters and particles of very small size (<1 nm) can be studied by mass spectrometry [25]. Optical diagnostics using Rayleigh-Mie scattering deal with observation of particles with larger size (diameter > 30 nm) [26]. It appears that intermediate size particles (protopowders) are not easy to characterise by Raighley-Mie scattering due to their small cross-section, and other techniques such as photodetachment [22] and laser-induced particle heating [27] are intrusive. A new, non-intrusive technique allowing the study of these protopowders is therefore of great interest.

It seems that the CRD technique is suitable for the study of powders in silane plasmas [10]. With this aim, we have performed measurements of the extinction coefficient in Ar/SiH_4 plasmas. For these experiments, the reactor

was heated at 200°C in order to reduce the powder formation rate [26]. By fitting the exponential decay time in real time for each laser pulse, we obtain the time evolution of the extinction coefficient after plasma ignition, as shown in figure 6 for different plasma conditions. In conditions of figure 6a), there was no decrease of the decay time after plasma ignition. In this case, the density of species present in the cavity and able to absorb or scatter the laser light (negative ions, powder,...) was below the detection limit.

In the other conditions, a decrease of the decay time was observed. At this stage, we cannot specify if the decrease is due to photodetachment on negative ions/clusters or scattering/absorption due to powder particles trapped in the plasma. The observed extinction coefficient is independent of the laser wavelength, in the dye range (510 – 620 nm). In figures 6b) and c), the observed slow oscillations of the extinction coefficient unambiguously indicate that the decrease of the decay time is due to solid particles created and trapped in the plasma. These oscillations are characteristic of powder creation/growth/elimination cycles in the reactor as already shown by other diagnostics [27]. At low silane dilution, as on figure 6d), the extinction coefficient rapidly reaches 5.10^{-5} cm^{-1}, after which, the ring-down signal is lost and no measurements are anymore possible. These results can be used to determine the measurable range of extinction coefficient in our system: the lower limit, about 10^{-8} cm^{-1} (10^{-7} cm^{-1} for real-time measurements) is determined by the shot-to-shot reproducibility of the laser, the dark noise of the detector, and other noise sources; the upper limit is about 5.10^{-5} cm^{-1}, when the decay time is shorter than the response time of our detection system.

It is important to notice that the CRD diagnostic presents a sensitivity of several orders of magnitude higher than a single pass absorption diagnostic. In the case of the cavity ring-down technique, we have observed extinction coefficients in the range 10^{-8}-5.10^{-5} cm^{-1}. A single path absorption arrangement allowing to detect transmitted relative intensity variations of about 10^{-3}, which represents a good signal/noise ratio, could not measure extinction coefficients less than about 10^{-4} cm^{-1} for our large reactor

The nature of species inducing the light absorption is difficult to determine. The extinction coefficient could be induced by a high density of small particles, or by a low density of large powder particles. At the laser wavelength (566 nm), only negatively charged clusters smaller than $Si_{10}H_x^-$ can be photodetached by the laser light [22]. The photodetachment cross-section of such clusters is known to be about $10^{-17}cm^2$. Therefore the clusters are observable if their number density is in the range 10^9-10^{12} cm^{-3}. In the case of larger particles (radius > 1 nm), the extinction of the light is due to absorption and Rayleigh scattering on particles and is given by the sum of absorption and scattering coefficients:

$$\alpha_{ext} = \alpha_{abs} + \alpha_{sca}$$

For relatively large particles (radius > 25 nm), the extinction is dominated by scattering of light by powder particles [28]. The scattering coefficient is given by:

$$\alpha_{sca} = 128.\pi^5.\left|(m^2-1)^2/(m^2+2)^2\right|.N_p.r^6/3.\lambda^4$$

For small particles (radius < 25 nm), the extinction is dominated by absorption of light by powder particles [28]. The absorption coefficient is given by:

$$\alpha_{abs} = 2\pi^2.Im(-(m^2-1)/(m^2+2)).N_p.r^3/\lambda$$

where λ is the laser wavelength, r is the average particle radius, m is the complex refractive index of the powder material, and N_p is the particle number density.

If we consider that particles are amorphous silicon, we admit that the complex refractive index is m = 4.4+0.3i [29] and the absorption cross-section of a 1 nm particle is about 10^{-17} cm^2. To be observable, such particles should present a number density in the range 10^9-10^{12} cm^{-3}. For larger particles (radius about 30 nm), the extinction is now dominated by scattering and the scattering cross-section is about 10^{-12} cm^2. The number density of such particles should be in the range 10^4-10^7 cm^{-3} to be within the detection limit of the present CRD arrangement. However, the number density of 30 nm particles in silane plasmas is generally larger than 10^9 cm^{-3} [30]. This indicates that the extinction observed in our argon/silane experiments is probably due

to small size particles (clusters or powders smaller than 30 nm). Since the detection of particles begins soon after plasma ignition, it is likely that the extinction of the signal intensity is due to a high density of small particles.

In the case of powder particles trapped in the reactor, the cavity ring-down technique allows to determine the volume fraction of the plasma occupied by solid-state particles. If we consider that powder consists of amorphous hydrogenated silicon, we admit a complex index m = 4.4 + 0.3i for the particles at the laser wavelength [29]. The volume fraction is given by $\Gamma = 4/3.\pi r^3.N_p$ ($\equiv V_{powders}/V_{plasma}$) [28]. In the range of our extinction measurements (10^{-8}-5.10^{-5} cm^{-1}), the volume fraction occupied by powder is therefore about 7.10^{-12} – $3.5.10^{-8}$. These values are much lower than the volume fractions measured in dusty plasmas by single-pass Mie scattering diagnostic (about 10^{-8} - 10^{-7}) [28]. It is important to note that the CRD technique complements the Rayleigh scattering technique, difficult to use when the volume fraction of solid powder within the plasma is small ($<10^{-8}$).

The cavity ring down technique has been used to observe absorption lines of SiH_2 radicals around 579 nm in plasmas [10]. In our experimental conditions, we have observe no absorption induced by SiH_2. In argon/silane mixtures, only few conditions avoided powder formation. These conditions were low input power and high silane/argon ratios (up to pure silane). It is evident that powder formation will prevent any spectral absorption measurements on the SiH_2 molecule. The ring-down time can be too low or perturbed by oscillations during the scan. When no powder is formed, no absorption peaks can be extracted from the noise. At low input power, the SiH_4 dissociation will be low and no SiH_2 will be observable. In high silane/argon ratios, silylene radicals are destroyed by association with silane molecules ($SiH_2+SiH_4->Si_2H_6$). Considering the mean free path at these pressures (about 1 mm), the silylene radicals are rapidly destroyed and are not observable. It is noticeable that we have observed argon absorption lines at 577.212 nm and 583.426 nm in pure argon plasmas. As a consequence, SiH_2 absorption lines cannot be extract from the noise because the density is

too low to induce observable absorption. We can therefore determine a higher limit for the SiH_2 density: since the noise corresponds to an extinction of about a few 10^{-8} cm^{-1}, this corresponds to a density of about 10^8 cm^{-3}.

To summarise, these results show that the CRD technique is a powerful, non-intrusive diagnostic for nanometric particles detection in dusty plasmas and can be used to investigate the early phases of powder formation and the coagulation of the protoparticles. Moreover, the cavity ring-down diagnostic could be of great interest as a monitor in industrial processes which require conditions free of nanometric particles to avoid contamination of sub-micron features.

c) Observation of a drift of the decay time during experiments

During these experiments, we frequently observed a spurious drift of the ring-down time induced by the presence of a plasma in the reactor. The typical behaviour of this drift is shown on figure 7. Before plasma ignition, the decay time is stable. When the plasma starts, the decay time decreases by about several microseconds, depending on the plasma type and duration. After plasma extinction, the decay time does not immediately return to its initial value but slowly recovers during several hours, even if the reactor is evacuated. This drift occurred in argon, hydrogen and oxygen plasmas, and was particularly noticeable in argon plasmas which should not have any effect on the ring-down decay time at 566 nm (no absorption lines). Clearly, meaningful measurements could not be made under such conditions. In cavity ring-down experiments, other authors have also found it necessary to run a plasma in the reactor for several hours, in order to stabilise the cavity [31].

The drift of the decay time is unlikely to be due to a degradation of the mirror reflectivity caused by heating of the mirror dielectric surface by plasma species such as ions and metastable atoms, because the distance between the plasma and the mirror surface is more than 35 cm. This is much larger typical mean free path length at 0.1 Torr (about 1 mm), and the solid angle of plasma seen by the mirror is small. Moreover, the drift is not due to particles

or desorbed species which were trapped in the plasma, because then the decay time should have reached its initial value immediately after reactor evacuation.

Several observations support the view that the degradation of the cavity ring-down time is in fact due to plasma desorption of species adsorbed on the reactor electrodes and walls, which then recondense on other surfaces, such as mirrors. This would reduce the mirror reflectivity and lead to the observed decrease of the decay time τ. This is not to be confused with accidental exposure of mirrors to oil vapour backstreaming from the pumps which causes immediate and permanent degradation of ring-down time, which can only be recovered by removing and cleaning the mirrors.

We assume that the main species involved here is water physisorbed on the reactor walls. This hypothesis is confirmed by the following observations. The drift is minimised when the base pressure in the reactor is low ($< 1.10^{-6}$ Torr), after prolonged pumping and heating at 200°C, i.e. after a thorough degassing of the reactor (see fig. 7). The plasma-induced drift decreases with time, and eventually disappears. But the drift reappears immediately if the reactor is opened to atmosphere and then evacuated. This is also consistent with the necessity of pumping the reactor slowly to avoid water condensation on the mirrors [8]. Finally, we note that the drift effect is worse in large area reactors than in small laboratory reactors, presumably because more water is desorbed from the larger surfaces.

No drift was observed during the powder experiments in Ar/SiH_4 mixtures, which suggests that the thin silicon film deposited on the reactor walls acts as a passivation layer. The adsorbed water is supposed to be trapped at the reactor surface and/or in the silicon film, and subsequently cannot be desorbed by the plasma. In order to test this hypothesis, the drift during the ignition and the extinction of an argon plasma was measured, before and after a silane plasma. Results are shown on figure 8. It is clear that a silane plasma running for 15 minutes reduces the ring-down time drift induced by the argon plasma. Moreover without silane plasma, it takes several hours to recover the initial cavity quality. But after silane plasma, the cavity recovers its initial state about 500 seconds after the argon plasma

extinction. In conclusion, reducing the drift is of great importance for CRD experiments. A deposition plasma (silane, for example) seems to limit or avoid the drift by passivating the reactor walls. Other solutions could be found in order to reduce the drift, for example, the mirrors could be heated in order to avoid water condensation on their surface.

The drift effect would appear to be a major limitation of the CRD technique, but it is merely a consequence of the diagnostic's high sensitivity to the presence of a thin film on the mirror surface. In fact, the CRD technique could be employed to study the optical/spectral characteristics of very thin films deposited on the mirror surface, for example at the early stages of a deposition process.

4. Conclusion

In conclusion, we have investigated the practicability of the cavity ring-down technique as a diagnostic for negative ions and powder particle detection in large area rf-plasma reactors. The negative ion densities found in pure oxygen and hydrogen plasmas (respectively about 10^{10}-10^{11} and 10^{9}–10^{10} cm^{-3}) are in good agreement with other experimental and numerical results. The observed spatial distribution is characteristic of negative ions trapped in rf plasmas. This shows unambiguously that the observed extinction is due to photodetachment on negative ions.

The cavity ring-down technique is a powerful technique for the characterisation of nano-scale particles created and trapped in dusty plasmas. The observed extinction due to the particles (10^{-7} to 5.10^{-5} cm^{-1}) is several orders of magnitude smaller than with other non-intrusive techniques (about 10^{-4} cm^{-1}). The time evolution of very low volume fractions of solid particles in the plasma (10^{-12} – 10^{-8}) can be measured by this technique.

One experimental difficulty is the plasma-induced drift of the decay time which can significantly perturb ring-down measurements. This drift is probably due to water desorption from the reactor electrodes and walls, which condenses on the mirror surfaces. Careful attention to reactor degassing is

sufficient to alleviate this problem. Also, a thin film of silicon reduces this drift probably by trapping the water between the reactor walls and the silicon layer. This film acts as a passivation layer.

The cavity ring-down technique is a powerful diagnostic for the characterisation of rf plasmas and could be extended to applications such as thin film characterisation or as industrial process control.

Acknowledgements

We thank L. Chevalley for participation in the measurements. This work was funded by Swiss Federal Research Grant BEW 9400051.

References

[1] A. O'Keefe and D. Deacon, Rev. Sci. Instrum. **59** (1988) 2544

[2] D. Romanini, "Cavity ring down and intracavity laser absorption" in "Cavity-RingDown Spectroscopy – a new technique for trace absorption measurements", 1-19, K.W. Busch and M.A. Busch eds., American Chemical Society, Washington, 1998

[3] A. O'Keefe, J.J. Sherer, A.L. Cooksy, R. Sheeks, J. Heath and R.J. SayKally, Chem. Phys. Lett. **172** (1990) 214

[4] T. Yu and M.C. Lin, J. Am. Chem. Soc. **115** (1993) 4371

[5] G. Meijer, M.G.H. Boogaarts, R.T. Jongma, D.H. Parker and A.M. Wodtke, Chem. Phys. Lett. **217** (1994) 112

[6] P. Zalicki, Y.Ma, R.N. Zare, E.H. Wahl, J. Dadamio, T.G. Owano and C.H. Kruger, Chem. Phys. Lett. **234** (1995) 269

[7] M. Kotterer, J. Couccicao and J.P. Maier, Chem. Phys. Lett. **259** (1996) 233

[8] D. Romanini and K.K. Lehmann, J. Chem. Phys. **99** (1993) 6287

[9] D. Romanini, A.A. Kachanov, N. Sadeghi and F. Stoeckel, Chem. Phys. Lett. **264** (1997) 316

[10] A. Campargue, D. Romanini and N. Sadeghi, J. of Phys. D, Appl. Phys. **31** (1998) 1168

[11] E. Quandt, H.F. Döbele and W.G. Graham, Appl. Phys. Lett. **72** (1998) 2394

[12] L. Sansonnens, A. Pletzer, D. Magni, A.A. Howling, Ch. Hollenstein and J.P.M. Schmitt, Plasma Sources Sci. Technol. **6** (1997) 170

[13] M.A. Lieberman and A.J. Lichtenberg "Principles of plasma discharges and materials processing" Wiley-Interscience Publications, New York, 1994

[14] D. Vender, W.W. Stoffels, E. Stoffels, G.M.W. Kroesen and F.J. de Hoog, Phys. Rev. E **51** (1995) 2436

[15] N. Yasuda, H. Amemiya and M. Endo, Proc. 2nd International Conference on Reactive Plasmas and 11th Symposium on Plasma Processing. p613, Yokohama, Japan, 1994

[16] T. Suzuki and T. Kasuya, Phys. Rev. A **36** (1987) 2129

[17] M. Shibata, N. Nakano and T. Makabe, J. of Phys. D Appl. Phys. **30** (1997) 1219

[18] M. Shibata, N. Nakano and T. Makabe, J. Appl. Phys. **77** (1995) 6181

[19] E. Stoffels, W.W. Stoffels, D. Vender, M. Kando, G.M.W. Kroesen and F.J. de Hoog, Phys. Rev. E **51** (1995) 2425

[20] J.P. Boeuf and L.C. Pitchford, Phys. Rev. E **51** (1995) 1376 and Kinema Research Associates SIGLO-RF (Simulation of Glow Discharges RF-excited, capacitively-coupled) modeling software

[21] J.H. Fink, Fusion Technology, **6** (1984) 548

[22] T. Fukuzawa, K. Obata, H. Kawasaki, M. Shiratani and Y. Watanabe, J. Appl. Phys. **80** (1996) 3202

[23] H. Müller et al., to be submitted to Plasma Sources Science and Technology

[24] K.G. Spears, T.J. Robinson and R.M. Roth, IEEE Trans. Plasma Sci. **14** (1986) 179

[25] A.A. Howling, C. Courteille, J.-L. Dorier, L. Sansonnens and Ch. Hollenstein, Pure Appl. Chem. **68** (1996) 1017

[26] J.-L. Dorier, Ch. Hollenstein and A.A. Howling, J. Vac. Sci. Technol. A **10** (1992) 1048

[27] A. Bouchoule, A. Plain, L. Boufendi, J.-Ph. Blondeau and C. Laure, J. Appl. Phys. **70** (1991) 1991

[28] C. Courteille, Ch. Hollenstein, J.-L. Dorier, P. Gay, W. Schwarzenbach, A.A. Howling, E. Bertran, G. Viera, R. Martins and A. Macarico, J. Appl. Phys. **80** (1996) 2069

[29] "Properties of Amorphous Silicon" published by INSPEC, London,1989, 328

[30] J.-L. Dorier, Ch. Hollenstein and A.A. Howling, J. Vac. Sci. Technol. A **13** (1995) 918

[31] C.H. Kruger, T.G. Owano, C.O. Laux and R.N. Zare, J. Phys. IV **7** (1997) 67

Figure captions

Fig. 1: Experimental set-up. The mirrors are outside the plasma and attached by tubes to the reactor side walls. The mirrors can be displaced vertically via a sliding vacuum sealed system.

Fig. 2: Extinction coefficient profile/O^- density vs the distance between the electrodes for different rf plasma powers (0.1 Torr, 100 sccm O_2).

Fig. 3: O^- density vs rf plasma power at different pressures at a gas flow of 100 sccm.

Fig. 4: Comparison of measured and calculated O^- density profiles (0.1 Torr, gas flow 100 sccm). The horizontal error bars are given by the laser beam diameter, the vertical error bars by the observed shot-to-shot variation in the measurements.

Fig. 5: H^- density vs plasma power for different pressures (gas flow 300 sccm).

Fig. 6: Time evolution of the extinction coefficient due to powder particles in Ar-SiH_4 plasmas at different conditions.

Fig. 7: Time-resolved measurements of the drift caused by an argon plasma (0.1 Torr, 200 sccm, 50 W) before and after 5h of degassing at 200°C.

Fig. 8: Time-resolved measurements of the drift caused by an argon plasma (0.1 Torr, 200 sccm, 50 W) before and after exposure to a pure silane plasma (15' duration, 0.2 Torr, 100 sccm, 50 W).

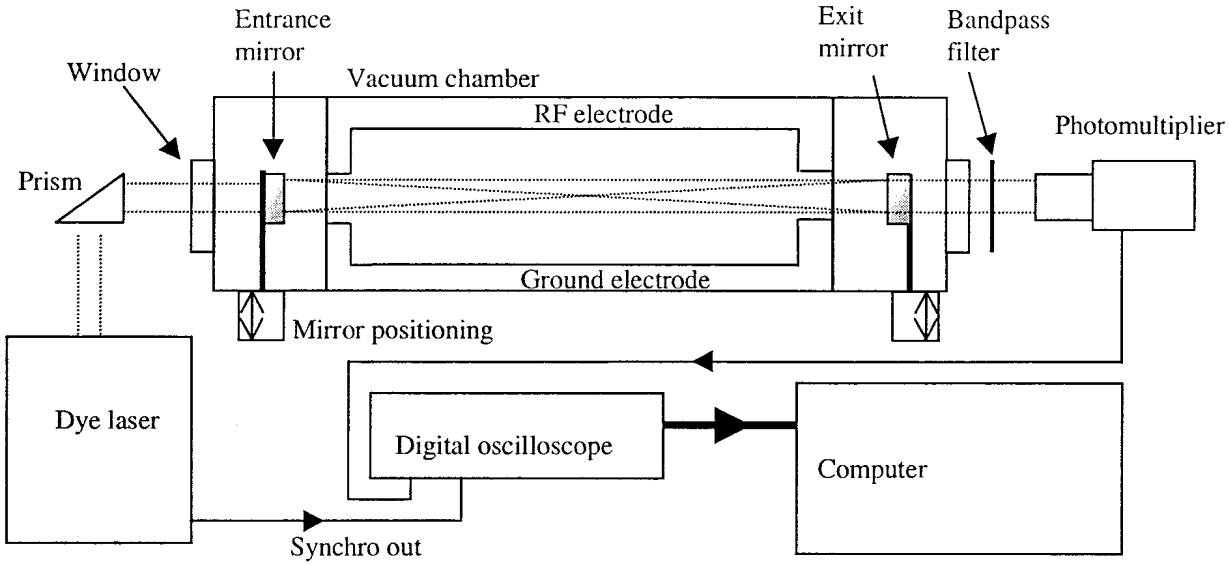

Fig. 1/8

F. Grangeon et al. "Applications of the cavity ring-down…"

Fig. 2/8 F. Grangeon et al. "Applications of the cavity ring-down..."

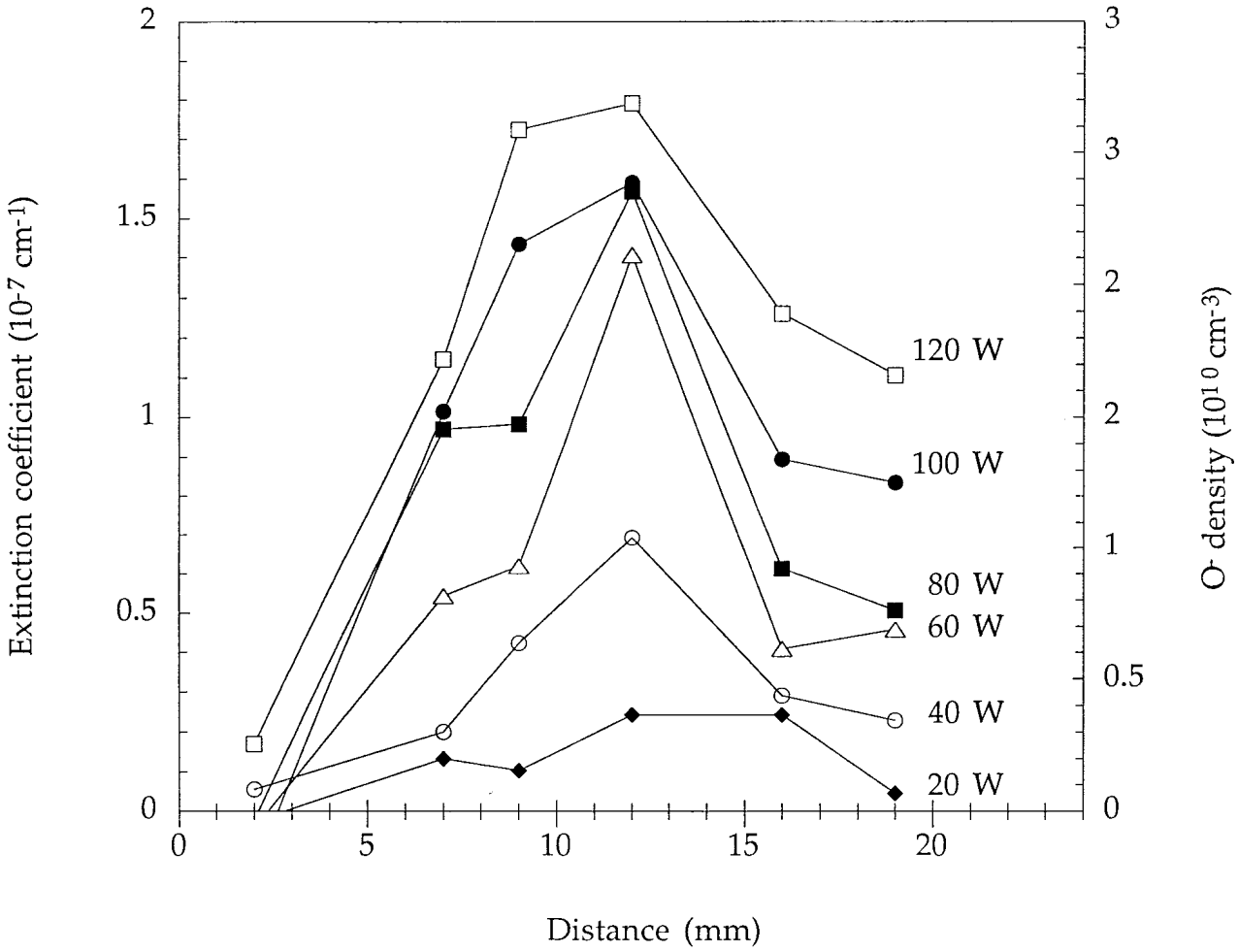

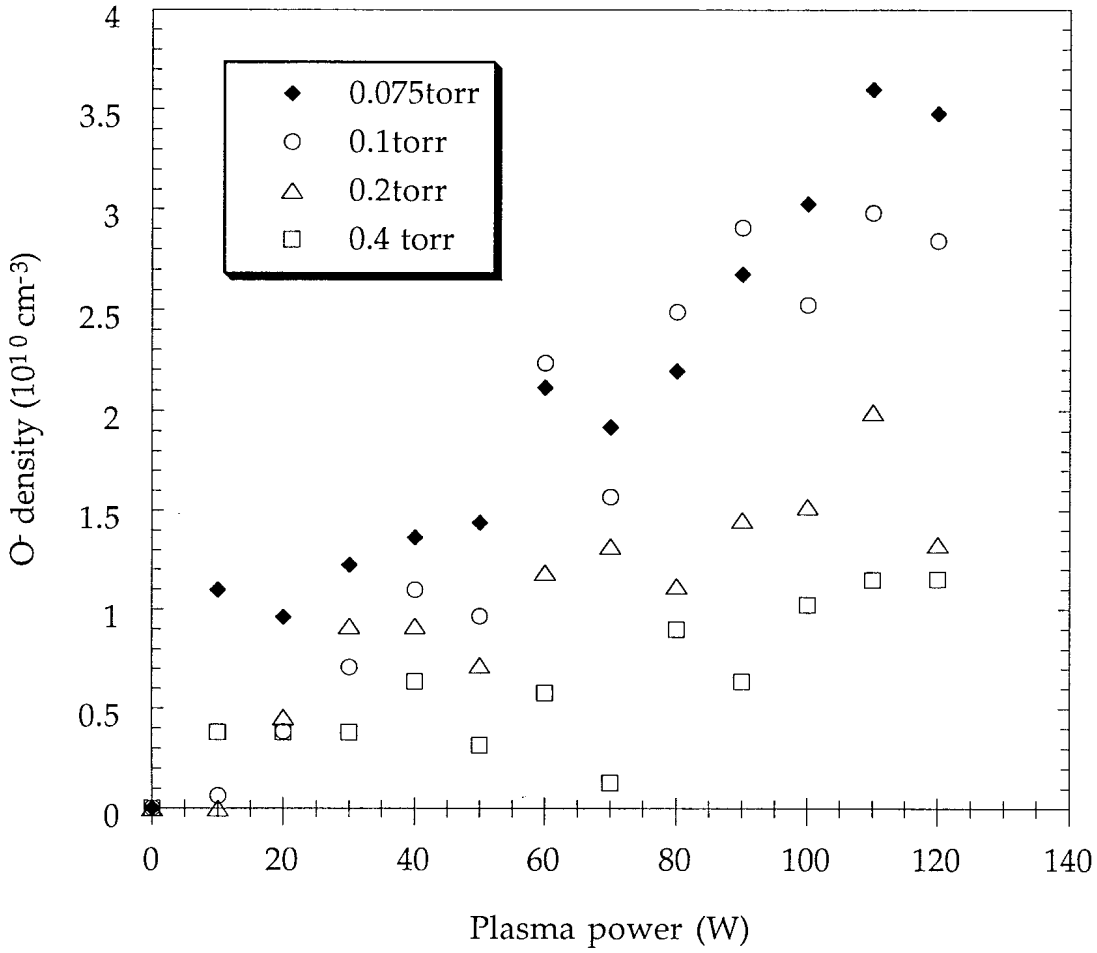
0.075torr
0.1torr
0.2torr
0.4 torr
O- density (10^{10} cm^{-3})
Plasma power (W)
0
0.5
1
1.5
2
2.5
3
3.5
4
0
20
40
60
80
100
120
140

Fig. 4/8 F. Grangeon et al. "Applications of the cavity ring-down..."

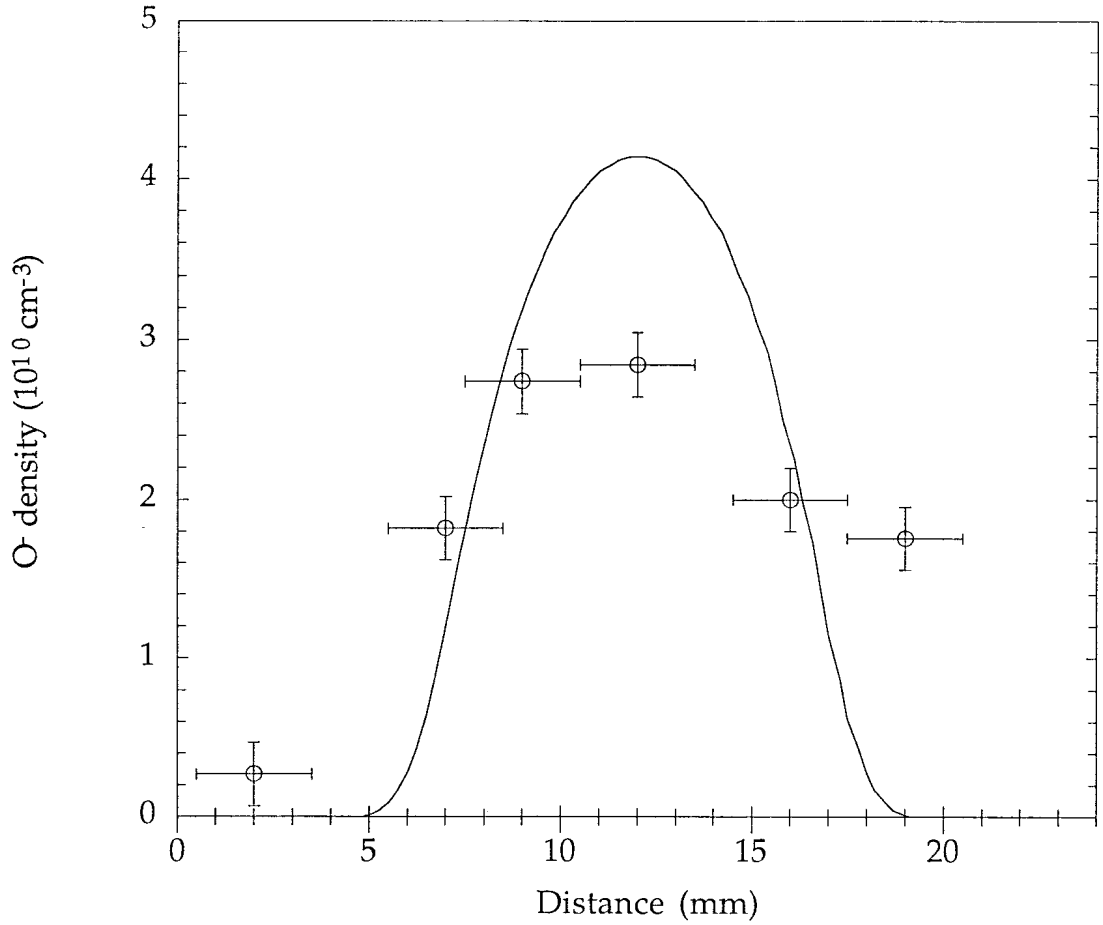

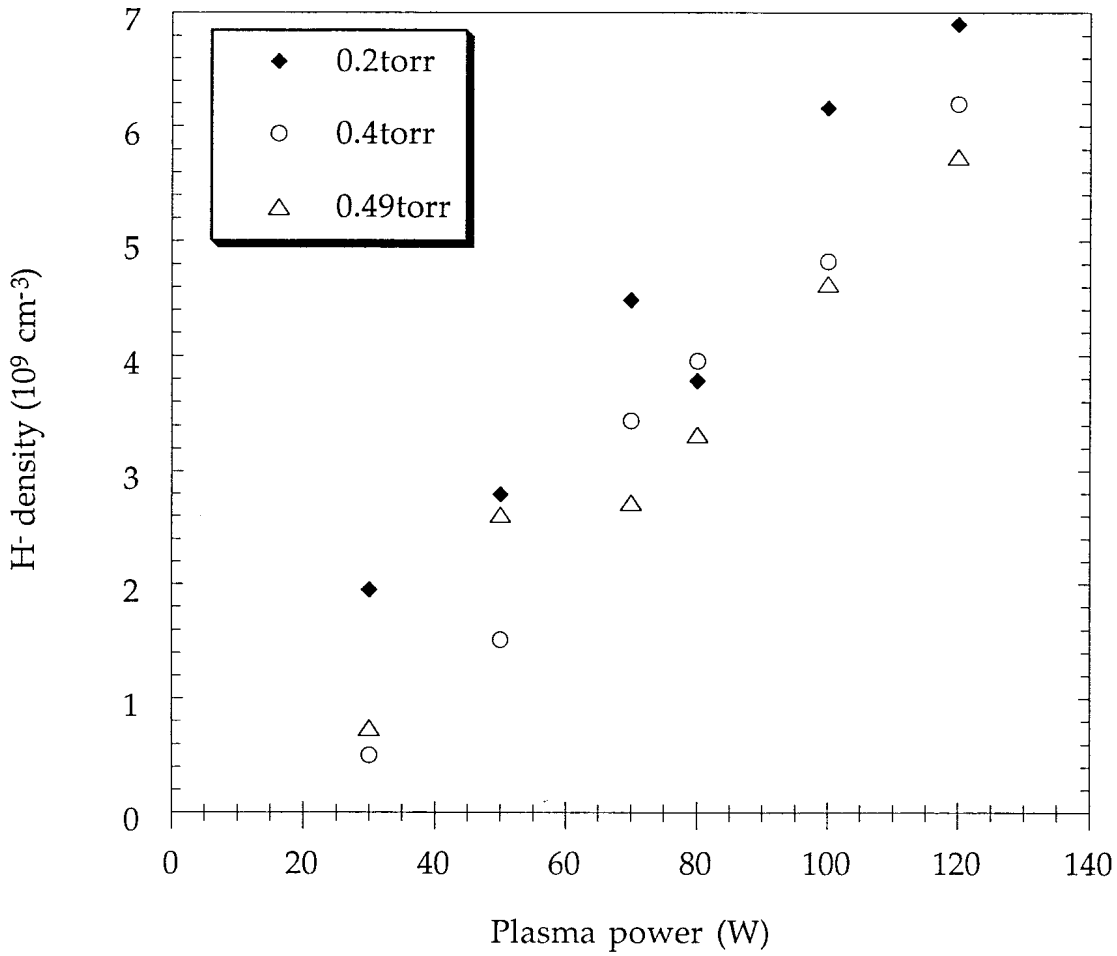
0.2torr
0.4torr
0.49torr
H- density (10^9 cm^{-3})
Plasma power (W)
0
1
2
3
4
5
6
7
0
20
40
60
80
100
120
140

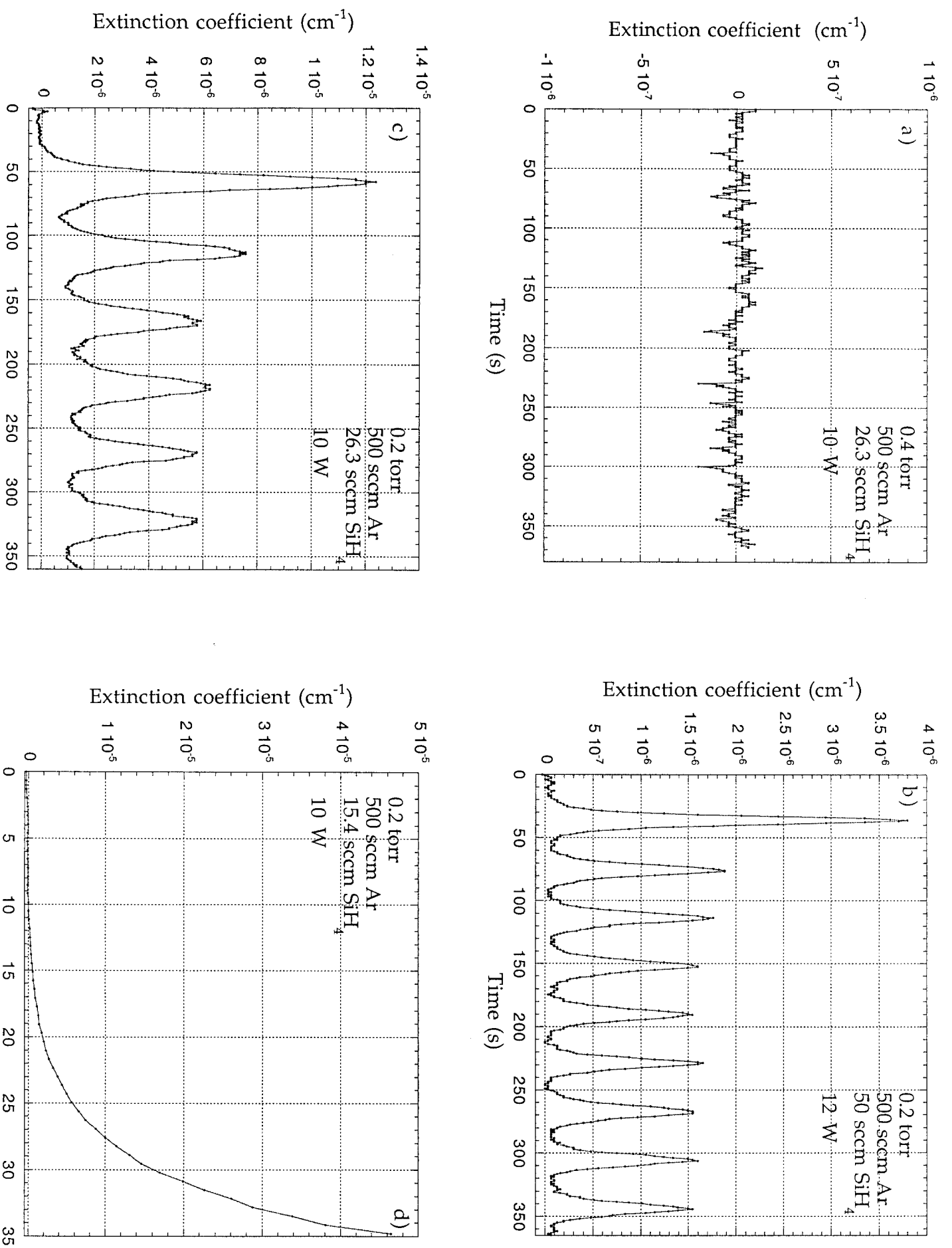

F. Grangeon et al. "Applications of the cavity ring-down..."

Fig. 6/8

Fig. 7/8

F. Grangeon et al. "Applications of the cavity ring-down..."

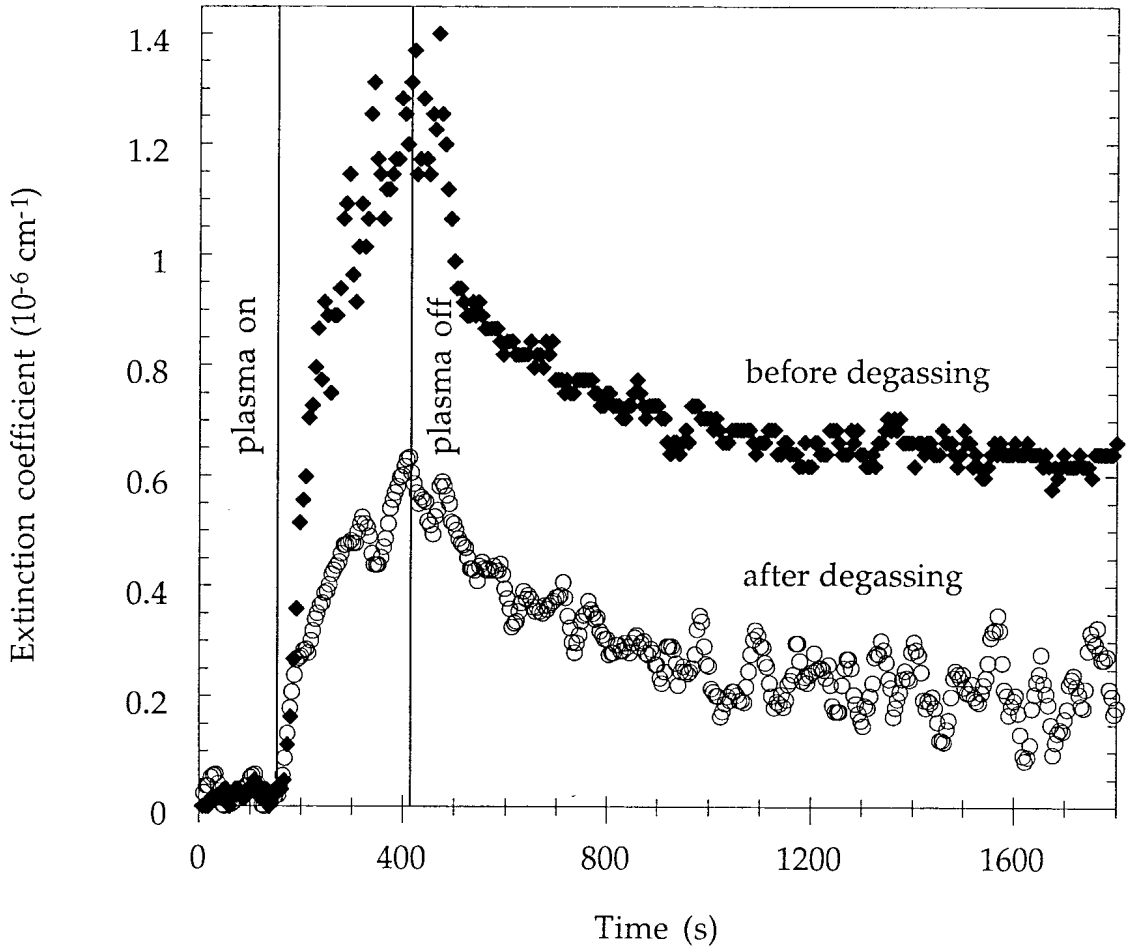

Fig. 8/8 F. Grangeon et al. "Applications of the cavity ring-down..."